Iranian Journal of Pharmaceutical Sciences
2022: 18 (3): 192-213
www.ijps.ir

Original Article

Antioxidant Effects of Amino Acids-Capped Silver Nanoprisms Against Cadmium-Induced Toxicity

Sarwar Allah Ditta[a,*], Atif Yaqub[a], Arslan Haider[a], Fouzia Tanvir[b], Muhammad Rashid[a]

[a]*Department of Zoology, Government College University, Lahore, Pakistan,* [b]*Department of Zoology, University of Okara, Okara, Pakistan.*

Abstract

The surface functionality of nanomaterials (NMs) with suitable biomolecules may enhance their biocompatibility and make them more effective for biological applications. Furthermore, the functionalization of various materials with biomolecules would also yield more secure and biocompatible nanomaterials for different applications. The present research was designed to evaluate the amino acids-based surface functionality of silver nanoprisms (AgNPrs). Silver nanoprisms were prepared by chemical method and further capped with amino acids such as L-cystine (Cys), L-glycine (Gly), and L-tyrosine (Tyr). Characterization of the newly-synthesized NMs was performed by using various techniques. Prepared nanomaterials (NMs) were assessed for their *in vitro* antioxidant activity using diphenylpicrylhydrazyl (DPPH), ferric reducing power (FRP), and hydrogen peroxide (HP) scavenging assays. *In vivo,* the antioxidant potential of the same was evaluated in the cadmium-intoxicated *Mus musculus* model. Tyr-AgNPrs ($p < 0.05$), Cys-AgNPrs ($p < 0.05$), and Gly-AgNPrs ($p > 0.05$) showed enhanced DPPH scavenging activity. Whereas the Cys-AgNPrs displayed enhanced FRP activity and Tyr-AgNPrs displayed enhanced HP scavenging activity. The AgNPrs and cadmium-exposed mice displayed a decreased ($p<0.05$) catalase (CAT) activity in G2 and G3, whereas it increased in G4. The superoxide dismutase (SOD) activity was decreased in the G2 ($p < 0.05$) and G5 ($p > 0.05$) groups, whereas it increased in the G3 ($p < 0.05$), G4, and G6 groups of mice. The G2 showed a slightly decreased glutathione-s-transferase (GST) activity ($p > 0.05$). The levels of reduced glutathione ($p<0.05$) and metallothioneins ($p>0.05$) were elevated in the cadmium-intoxicated group. The results revealed that the cystine-AgNPrs and tyrosine-AgNPrs demonstrated higher antioxidant potential in comparison to other treatments. It is concluded that biomolecule-conjugated AgNPrs can work efficiently with more biocompatibility for various nanotechnological and biomedical applications.

Keywords: Amino acids, Silver nanoprisms (AgNPrs), Oxidative stress, Glutathione, Metallothioneins (MTs), Antioxidant NPs.

1. Introduction

A remarkable revolution and uprising have taken place in nanoparticle innovations and nanotechnology over the last two decades [1]. Nowadays, nanoparticles (NPs) are largely utilized in various consumer products. Metallic NPs, especially Nobel metal NPs, have obtained valuable considerations because of their unique optical and physicochemical properties, which largely depend upon the shape and size of the NPs. These entities are

Corresponding Author: Sarwar Allah Ditta, Department of Zoology, Government College University, Lahore 54000, Pakistan. Tel: (+92) 32 34666709, E-mail: sarwar.mini@yahoo.com
Cite this article as: Ditta SA, Yaqub A, Haider A, Tanvir F, Rashid M., Antioxidant Effects of Amino Acids-Capped Silver Nanoprisms Against Cadmium-Induced Toxicity, Iran. J. Pharm. Sci., 2022, 18 (3): 192-213.

also important for their colorimetric sensing ability for various analytes [2-5].

Different shapes of Silver NPs portray unique physicochemical properties for a variety of reactions. Among all shapes of silver NPs, silver nanoprisms (AgNPrs) are considered for their exceptional and notable optical properties. Unique features of AgNPrs make them the best fit for biomedical research and exploration. These features are important in the development of novel biosensors [6, 7], affinity sensors [8, 5], signal transducers [9-11], biomimetic molecules [12, 13], antibacterial [14], and antioxidant NPs for different biomedical devices.

The unique features of NPs make them attractive materials for diagnostic [15, 16] and therapeutic applications [17]. However, using these NPs for biomedical applications or as nanomedicine demands their controlled and regulated interactions with different biomolecules [18, 19]. Tailored NPs with improved payload binding capability and reduced cytotoxicity may enhance the cellular internalization of NPs [20]. Similarly, surface functionality may alter the surface properties of NPs in different ways to make them ideal for specific or selective recognition for different biomedical applications [18, 21, 5]. Even surface functionality may also alter the specific immune response to NPs in the animal body [22, 23].

Specific ligands may impart specific properties to the NPs on functionalization. Amino acids are among the naturally available low-cost and biocompatible compounds, which can provide effective functionality to the NPs depending upon their low toxicity and residue conformation [24, 25]. Amino acids generally provide a long hydrophobic tail (alkyl chain) and a hydrophilic head (charged amino acid) [24]. Amino acids-based surface functionality has been the subject of many studies, because of their enormous impending applications in food, cosmetic, pharmaceutical, and household products [26, 27]. Different studies have reported amino acids-mediated functionalization of metallic NPs for various applications [28-32]. According to the information we have, there is no study previously described on amino acid-based functionalization of AgNPrs for their altered oxidative potential in animal exposure studies. In the present study, AgNPrs were synthesized and functionalized with selected L-amino acids, as the L-amino acids are mostly used in protein biosynthesis in animal bodies. The resultant nanoprisms were characterized and assessed for their altered *in vitro* and *in vivo* antioxidant properties.

2. Materials and Methods

2.1. Chemicals and Reagents

All the amino acids were procured from Merck and were used as obtained. Sodium borohydride ($NaBH_4$), Iron (III) chloride, silver nitrate ($AgNO_3$), polyvinylpyrrolidone (PVP) (average molecular weight 40,000), potassium hexacyanoferrate (III) ($K_3Fe(CN)_6$), pyrogallol, trisodium citrate ($Na_3Cit.2H_2O$), trichloroacetic acid (Cl_3CCOOH), 5,5′-Dithiobis (2-nitrobenzoic acid) (DTNB), and 2, 2-diphenyl-1-picrylhydrazyl were purchased from Sigma Aldrich, USA. In

addition, β-Mercapto-ethanol (purity ≥99.0%), phenyl methyl sulfonyl fluoride (PMSF) (purity >99%), reduced glutathione (purity ≥98.0%), and all other chemicals were purchased from best vendors and used as delivered.

2.2 Synthesis of AgNPrs

Synthesis of AgNPrs was accomplished as per the protocol of previously published reports [33, 34]. In a 250 mL sterilized flask, the following chemicals were added in order: 2 mL silver nitrate (0.37 M), 2.5 mL trisodium citrate (12.5 mM), and 1.5 mL hydrogen peroxide (30% by weight) alongside constant agitation. The volume of the solutions reached 100 mL with deionized (DI) water. After 10 minutes of continuous agitation at 40 °C, 3 mL sodium borohydride (5 mM) was added dropwise. As the reaction proceeded, shifts in color were observed from transparent to light yellow to dark, which eventually changed to blue color. The change in sodium borohydride concentration produces a variety of colors, which indicate the different sizes of formation of AgNPrs. Stable AgNPrs was obtained after about 3 minutes, purified, and stored.

2.3. Fabrication of nanoconjugates

The AgNPrs was capped with L-tyrosine, L-cystine, and L-glycine, as per previously reported methods [35, 36]. Briefly, amino acid-conjugated AgNPrs was developed by the conjugation of selected amino acids onto the PVP-stabilized AgNPrs under constant stirring. Change in the original color of chemically synthesized AgNPrs was taken as an indicator of capping. The solution was centrifuged at 13000 rpm for 15 minutes and the pallet was resuspended in deionized (DI) water.

2.4. Characterization of nanoprisms

The synthesized materials were characterized by utilizing different facilities such as zeta potential (Zeta sizer Nano ZS-90-Malvern Instruments, Malvern, UK), Fourier-transform infrared spectroscopy (FTIR) (Shimadzu IR Prestige 21), UV-visible (UV-Vis) spectroscopy (AE-S70-1U), etc. Zeta potential (ZP) values generally describe the net surface charges and stability of NPs, while FTIR analyses describe the functional groups involved in synthesis process. While ultraviolet-visible spectroscopy is a widely applied technique for assessing and evaluating the growth, stability, and applications of nanomaterials.

2.5. In vitro antioxidant activity

The DPPH scavenging activity of AgNPrs and its conjugates was assessed by using previously reported protocols [37-39, 32]. DPPH scavenging activity was estimated using Equation 1. Ferric reducing power (FRP) activity of NMs was evaluated by using previously reported methods with slight modifications [40, 32]. Briefly, different concentrations of samples (1.0 mL, 50-200 µg/mL) were mixed with phosphate buffer (2.5 mL, 200 mM, pH 6.6) and $K_3Fe(CN)_6$ (2.5 mL, 1% w/v) and incubated (25 min, 50 °C). Then, centrifugation (3000 rpm, 10 min) was

performed after the addition of trichloroacetic acid (2.5 mL, 10% w/v).

Then, the supernatant (2.5 mL) was added with distilled water (2.5 mL) and ferric chloride ($FeCl_3$) (0.5 mL, 0.1% w/v). The absorbance of the samples was taken at 700 nm against a blank sample (**Table 1**). The hydrogen peroxide (HP) scavenging activity of AgNPrs was calculated by using the protocol of Keshari *et al.* (2016) [41]. The HP scavenging % was evaluated by using equation 1.

$$\% \text{ of Scavenging} = (Pc\text{-}Ps/Pc) \times 100 \quad \text{(equation 1)}$$

Where Pc= absorbance of control and Ps= absorption of the sample

Table 1: Concentrations and volume of reagents for ferric reducing power assay.

Reagents	Test (µl)	Control (µl)
Sample/Serum	1.0 mL	-
Distilled water	-	1.0 mL
0.2 M Phosphate Buffer	2.5 mL	2.5 mL
K_3 Fe $(CN)_6$ (1% w/v)	2.5 mL	2.5 mL
Incubation (at 50°C for 20 min)		
Trichloroacetic acid (10%)	2.5 mL	2.5 mL
Centrifugation (3000 rpm, 10mints) supernatant (2.5 mL) collection		
Distilled Water	2.5 mL	2.5 mL
$FeCl_3$ (0.1%)	0.5 mL	0.5 mL
Measure OD at 700 nm		

2.6. In vivo animal trials

Swiss albino mice (female and male, average body weight (BW)=30-35 g, age=8-10 weeks old) were obtained from Animal House of Government College University Lahore, Pakistan. Experimental conditions (22±2°C temperature, 12h dark/light cycle) for animals were provided during the whole experiment. Animal handling ethical guidelines was obtained and approved by the designated committee of Government College University Lahore for animal trials. All animals were acclimatized for one week before experiment. The animals were provided with a standard mouse diet pellet and were supplied with a water source (*ad libitum)*. Six groups of mice were formed (G1-G6) containing five animals (n=5) per group. Where G1 was provided with saline water, G2 was fed with cadmium metal only (20 mg/kg of BW), G3 was provided with cadmium metal (20 mg/kg of BW) and C-AgNPrs (20 mg/kg of BW), G4 with cadmium metal (20 mg/kg of BW) and Tyr-AgNPrs (20 mg/kg of BW), G5 with cadmium metal (20 mg/kg of BW) and Gly-AgNPrs (20 mg/kg of BW), and G6 with cadmium metal (20 mg/kg of BW) and Cys-AgNPrs (20 mg/kg of BW) (**Table 2**). The

Table 2: All animals were treated (n = 5) and dosed for 28 days as per guidelines of Test No. 407 of OECD using oral gavage [42]. Where Cad; Cadmium metal, C-AgNPrs; chemically-synthesized silver nanoprisms, Tyr-AgNPrs; L-tyrosine-capped silver nanoprisms, Gly-AgNPrs; L-glycine-capped silver nanoprisms, Cys-AgNPrs; L-cystine-capped silver nanoprisms.

Groups	Treatment (s)
G1-Negative Control	Saline Water only
G2-Positive control	Cadmium (20mg/kg BW) only
G3-Treatment	Cadmium (20mg/kg BW) + C-AgNPrs (20mg/kg BW)
G4-Treatment	Cadmium (20mg/kg BW) + Tyr-AgNPrs (20mg/kg BW)
G5-Treatment	Cadmium (20mg/kg BW) + Gly-AgNPrs (20mg/kg BW)
G6-Treatment	Cadmium (20mg/kg BW) + Cys-AgNPrs (20mg/kg BW)

acute-toxicity study was performed using oral administration of test materials for 28 days according to the guidelines of the organization of economic cooperation and development (Test No. 407) (OECD, 2008) [42]. Mice were monitored and weighed regularly. After completion of the animal trial period, all animals were sacrificed, and blood samples and various body organs, i.e., liver, kidney, and intestine, were obtained and stored appropriately for analysis.

2.6.1. Endogenous antioxidant enzymes

Superoxide dismutase (SOD) was estimated by using a previously published method [43], and glutathione-s-transferase (GST) and catalase (CAT) activities were evaluated by using previously reported procedures [44].

2.6.2. Determination of reduced Glutathione

Reduced Glutathione (GSH) was estimated by using reported procedures [45, 32]. Samples were washed in KCl solution (150mM, chilled) and stored in liquid nitrogen immediately. A 10% tissue homogenate was prepared with distilled water (chilled). Tissue homogenate (10% w/v, 1.0mL) was added to trichloroacetic acid (10% w/v, 1.0mL, chilled). Then, incubation (10min, RT) and centrifugation (10min, 10000rpm) were performed. Then, 5, 5'-dithiobis-2-nitrobenzoic solution (pH 7.6, 1.25 mL, 5 mg/50 mL of 0.05M phosphate buffer) was added to the supernatant (0.25mL) and the mixture was further incubated (5min, RT). Finally, the absorbance of the mixture was measured at 405 nm. A standard curve of glutathione (freshly prepared) was used to evaluate the level of GSH in samples, and the results were described as mg of GSH per mg of protein.

2.6.3. Determination of Metallothioneins

Metallothioneins (MTs) were evaluated by using published methods [46, 47, 32]. Homogenate of samples was prepared in PMSF buffer. Then, the homogenate was centrifuged (15,000 x g, 30 min, 4°C), and the supernatant was added in ethanol-chloroform (1:1/ v: v), and further, the reaction and analysis were performed as per protocol (**Table 3**). Finally, the level of MTs was evaluated by using a standard curve (of glutathione), while considering 30 cystine residues per MT molecule.

Table 3: Reagents and their concentrations used during MTs analysis.

Sample/ Reagents	Volume (µl)
Homogenate supernatant-1	300
Ethanol-chloroform (1:1 / v:v)	342
Centrifugation (6000 x g, 10 minutes, 4° C)	
Supernatant-2	490
Ethanol-HCl (1:1 / v: v)	1.502
Incubation (1h, 20 ºC) and centrifugation (6000 x g, 10 minutes, 4 °C) and the resultant pellet was re-suspended	
NaCl (250 mM)	50
Sodium-EDTA (4 mM in 1M HCl)	50
Ellman's solution (2 mM DTNB, 0.2M Sodium phosphate, 2M NaCl)	1000
Centrifugation (3000 x g, 5 minutes, 4 °C)	
OD was recorded at 412 nm	

2.7. Data Analysis

For the normal data set, ANOVA with the Tukey test as post-hoc was performed, while for skewed data the Kruskal-Wallis H was used

followed by multiple comparisons. The data were analyzed by SPSS®. V22. Different other software platforms, such as ImageJ®, CorelDraw X4®, and Origin 2022®, were utilized to analyze the data.

3. Results and Discussion

3.1. Synthesis of AgNPrs and their Conjugates

3.1.1. Ultraviolet-visible Spectroscopy

Silver nanoprisms were synthesized by reacting silver nitrate and sodium borohydride in hydrogen peroxide as an etching agent. Initially, silver NPs were formed as the reaction proceeded, and the etching reaction of the hydrogen peroxide changed spherical NPs into prismatic triangles or AgNPrs. Two types of nanoprisms were synthesized, i.e., Large and small. Large nanoprisms were blue, while the smaller ones were purple. Blue AgNPrs (C-AgNPrs) exhibited three peaks, i.e., 980, 649, and 334 nm. The peak at 980 nm was very broad and hump-shaped, while the peak at 649 nm was not prominent as at 334 nm (**Figure 1a**). While purple-colored prisms displayed two prominent peaks, i.e., 635 and 337 nm, the third peak at 464 nm was not so prominent (**Figure 1b**).

Figure 1: UV-visible Spectroscopy of; *(a)* blue AgNPrs and their nanoconjugates, *(b)* purple silver nanoprisms.

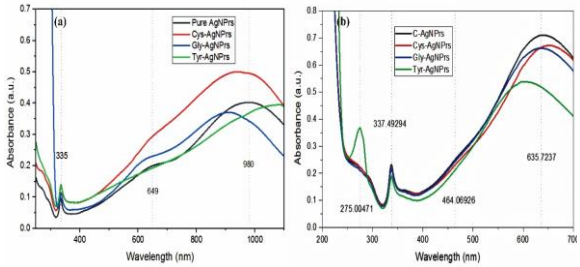

After conjugation with amino acids, all these peaks showed a red or blue shift in their UV-Visible peaks. In the case of L-cystine capped AgNPrs (Cys-AgNPrs) prominent peak was recorded at 970 nm (AE-S70-1U), while the second peak was recorded at 654 nm, and the third peak was observed at 335 nm. In L-glycine-capped AgNPrs (Gly-AgNPrs) main broader peak was recorded at 915 nm, while the second peak was at 632 nm, and the third peak was recorded at 335 nm. In L-tyrosine-capped AgNPrs (Tyr-AgNPrs) main broader peak was recorded at a value higher than 1093 nm. The second peak was almost negligible, while the third peak was recorded at 335 nm (**Figure 1a**). Chang in color and surface plasmon resonance (SPR) peaks values after conjugation indicated the successful conjugation (**Figure 1**). Optical properties of the nanoconjugates were also utilized to assess the successful generation of nanoconjugates, where the color of the solution characteristically changes after a specific reaction. The blue AgNPrs changed into various shades of blue color after reaction with different amino acids; Tyr-AgNPrs depicted a purplish-blue color, Gly-AgNPrs gave a deep clear blue color, while Cys-AgNPrs developed a dull-deep blue color (**Figure 2a**).

3.1.2. Visual properties and zeta potential of NMs

AgNPrs and its conjugates displayed slightly different colors with different values of zeta potential, i.e., -35.89 ± 1.14, -26.83 ± 1.78, -51.37 ± 1.01, and -61.46 ± 2.45 mV for C-AgNPrs, Cys-AgNPrs, Tyr-AgNPrs, and Gly-AgNPrs, respectively (**Figures 2a and 2b**).

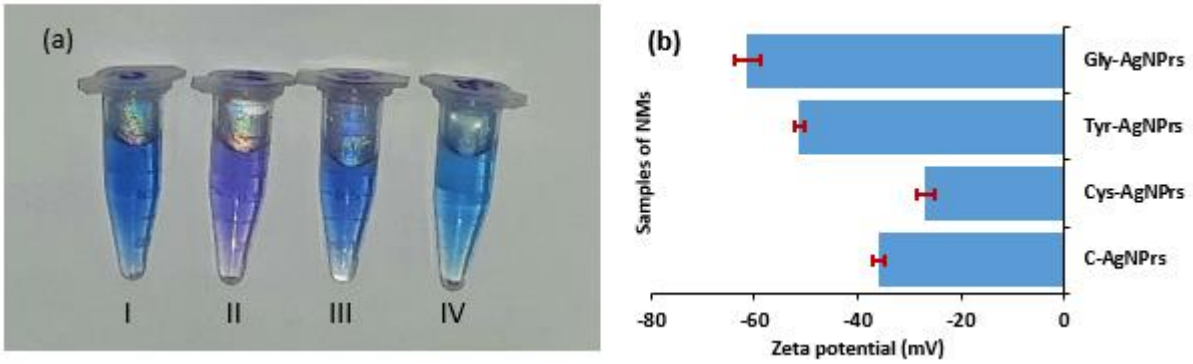

Figure 2. Characterization of AgNPrs, *(a)* AgNPrs and its conjugates, whereas; I= chemically-prepared NMs, II= Tyrosine-AgNPrs, III= Glycine-AgNPrs, IV= Cystine-AgNPrs, *(b)* Zeta potential values of AgNPrs and its nanoconjugates, *n = 3*.

3.1.3. Evaluation of functional groups through FTIR spectroscopy

The data of Fourier-transform infrared spectroscopy (FTIR) displayed successful capping of amino acids on the chemically-synthesized AgNPrs (**Figure 3**). After the synthesis of Cys-AgNPrs, different peaks of l-cystine were reduced or disappeared, i.e., 1230, 1377, 1516, 1749, and 2355 cm^{-1} corresponding to the presence of C-N, C-H, -C-C=C, C=O, and C=N, respectively (**Figure 3a**).

Several peaks of l-glycine, such as 1226, 1558, 1747, 2112, and 2355 cm^{-1}, corresponding to C-N, N-H, C=O, COOH, and C=N functional groups were seen reduced or disappeared (Fig. 3b). Followed by the formation of Tyr-AgNPrs, several peaks at 840, 1043, 2351, 2644, 2933, and 3207 cm^{-1} indicating to C-N, C=N, -OH, -N-H, and NH_2 were disappeared or reduced (**Figure 3c**).

3.1.4. Stability of AgNPrs and their conjugates

All the samples of AgNPrs and their conjugates were studied for their stability for up to one year by using UV-visible spectroscopy (**Figure 4**). Over time, all the samples showed an increase in absorbance values in their concerned peaks with redshift in their peaks (figures 4a, 4c & 4d) except for Cys-AgNPrs, where over time; one peak changed into two distinct peaks, indicating a change in the shapes of these nanoconjugates (**Figure 4b**).

3.2. Antioxidants activity of modified AgNPrs (in vitro)

3.2.1. DPPH assay

The original purplish color of DPPH converts to yellowish with the addition of strong antioxidants, while mild antioxidants induce a mild change in color and absorbance of DPPH at 517 nm. Chemically-synthesized AgNPrs (C-AgNPrs) did not exhibit any antioxidant activity. Instead, they showed concentration-dependent pro-oxidant activity. The Cys-AgNPrs and Tyr-AgNPrs showed modified antioxidant activity and displayed concentration-dependent antioxidant activity, whereby, Cys-AgNPrs showed more promising results at 100 µg/mL, i.e. 11.87 ± 6.74% than C-AgNPrs (-15.25 ± 10.55%), Gly-AgNPrs (5.75 ± 3.98%), and Tyr-AgNPrs (7.48 ± 5.25%) (**Figures 5a and 5b**).

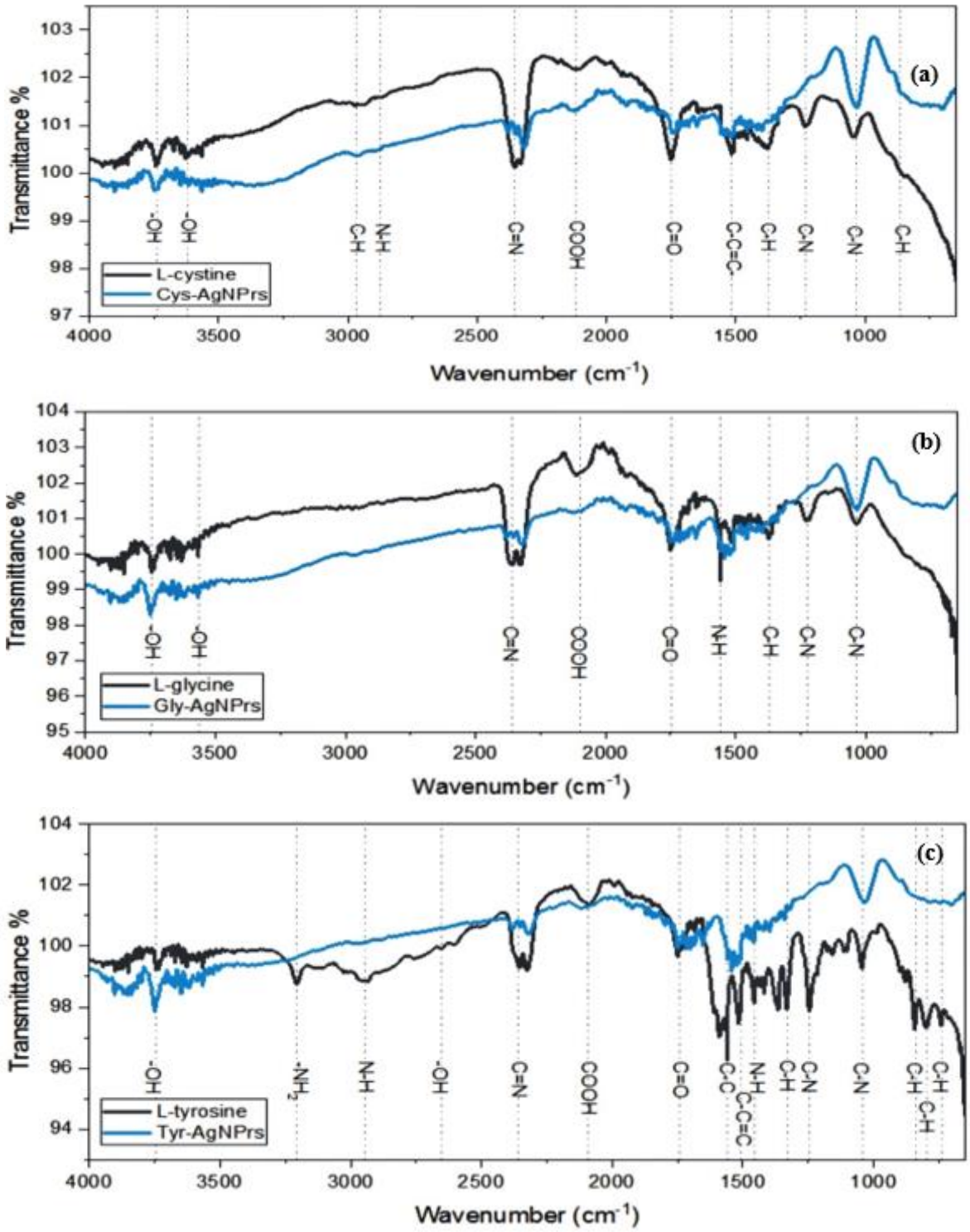

Figure 3. Fourier-transform infrared spectroscopy of; *(a)* L-cystine and Cys-AgNPrs, *(b)* L-glycine and Gly-AgNPrs, *(c)* L-tyrosine and Tyr-AgNPrs.

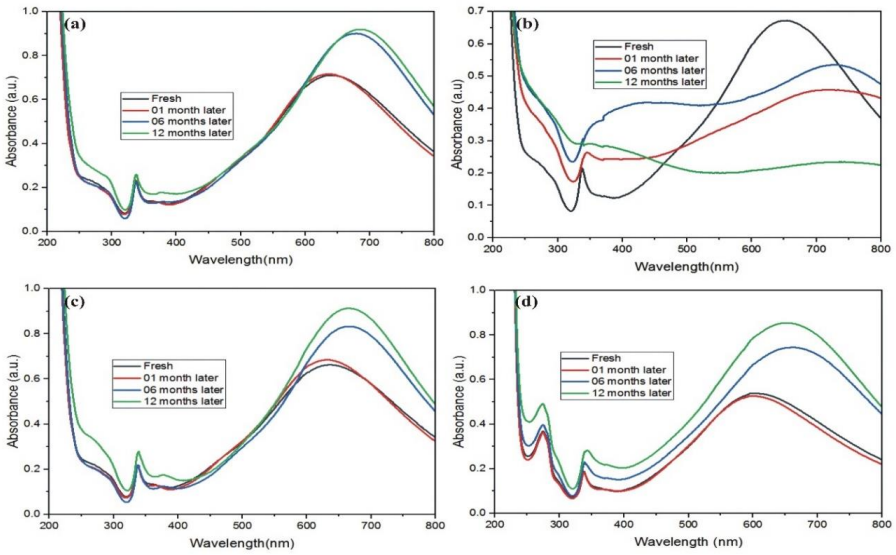

Figure 4. UV-Visible spectroscopy-based stability study of; *(a)* C-AgNPrs, *(b)* Cys-AgNPrs, *(c)* Gly-AgNPrs, *(d)* Tyr-AgNPrs.

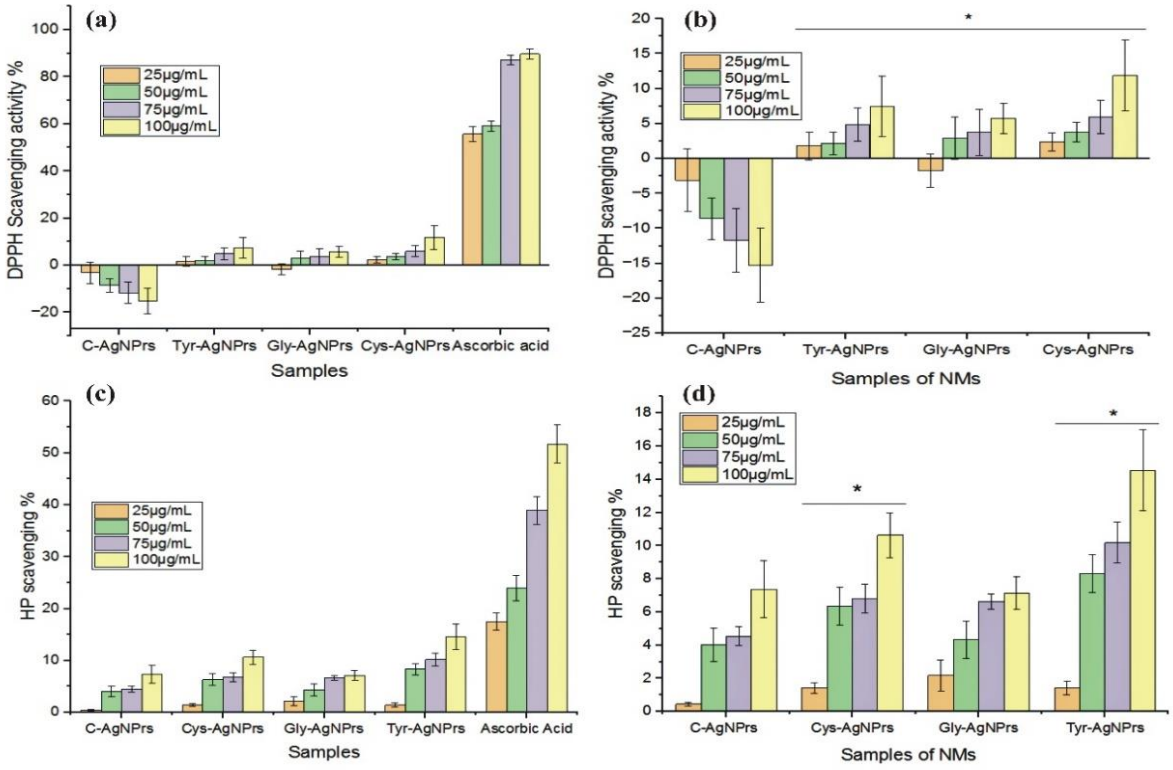

Figure 5. *In vitro* antioxidant activities of NMs; (*a)* DPPH scavenging activity of the AgNPrs in comparison with ascorbic acid, *(b)* DPPH scavenging activity of prismatic nanoconjugates. The data shown are Mean ± SD values with $n = 6$. For homogeneity of data ($p > 0.05$), a statistically significant difference was found in the DPPH scavenging activity of nanoconjugates of AgNPrs, Two-way ANOVA followed by posthoc Tukey test was conducted, where "*" indicates $p < 0.05$ when compared with C-AgNPrs, *(c)* HP scavenging activity of AgNPrs, amino acids-capped AgNPrs and ascorbic acid, *(d)* HP scavenging activity of AgNPrs and their nanoconjugates. The data shown are Mean ± SD values, $n = 3$, for homogeneity of data ($p > 0.05$), a statistically significant difference was found in HP scavenging activity of different conjugates, Two-way ANOVA followed by posthoc Tukey test was conducted, where "*" indicates $p < 0.05$ when compared with C-AgNPrs.

3.2.2. HP scavenging activity

Among all the AgNPrs and their amino acids capped-nanoconjugates, Tyr-AgNPrs and Cys-AgNPrs exhibited higher hydrogen peroxide scavenging % compared to C-AgNPrs and Gly-AgNPrs. Gly-AgNPrs also showed very minute HP scavenging activity compared to the other conjugates (**Figures 5c and 5d**).

3.2.3. Ferric reducing power (FRP) activity

Chemically synthesized AgNPrs and amino acid-capped AgNPrs were also assayed for FRP activity. Cys-AgNPrs exhibited higher FRP activity than all other nanoconjugates. Chemically-synthesized AgNPrs also demonstrated FRP activity, but it was less than the activity of Cys-AgNPrs but higher than Gly-AgNPrs. Here Tyr-AgNPrs displayed an inverse relationship between FRP activity and concentration, i.e., with the increase in concentration, the FRP activity of Tyr-AgNPrs decreased (**Figure 6**).

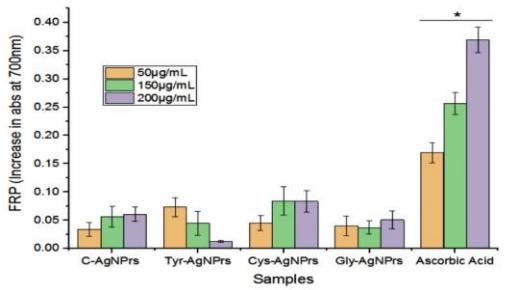

Figure 6. Ferric reducing power assay of AgNPrs and its conjugates, the data shown are Mean ± SD values with $n = 3$. For homogeneity of data $p > 0.05$, different nanoconjugates showed a statistically significant difference in FRP ($df_{6, 24}$; mean square = 0.002; $F = 6.05$; partial $\eta^2 = 0.60$ and $p < 0.05$), Two-way ANOVA with posthoc Tukey test was conducted, where "*" indicates $p < 0.05$.

3.3. In vivo Antioxidant Activity of silver nanoprisms

In-vivo antioxidant potential of AgNPrs was assessed by evaluating superoxide dismutase (SOD), reduced glutathione (GSH), catalase (CAT), glutathione-s-transferase (GST), and metallothioneins (MTs) in different tissues (**Table 5**).

3.3.1. Bodyweight

A slightly increased in body weight (BW) of mice was recorded in all the experimental groups (**Figure 7a**, **Table 4**). All animals appeared to be fine and stable through the entire trial period except for one mouse in the G3 group that developed a shoulder tumor.

3.3.2. Endogenous enzymes in exposure to AgNPrs

The Catalase (CAT) activity in the liver tissues was reduced ($p<0.05$) in the G2 and G3 groups of mice, however, it was elevated in the G4 group. While, CAT activity in serum samples was elevated ($p<0.05$) in group G3 and G4 and non-significantly increased in the G5 group, while the G2 group showed decreased ($p>0.05$) CAT activity (**Figure 7b**).

The SOD activity in the liver samples was reduced in G2 ($p<0.05$) and G5 ($p>0.05$) groups, while it was increased in G3 ($p<0.05$), G4, and G6. Whereas in serum samples, G2 and G5 groups demonstrated significantly decreased ($p < 0.05$) SOD activity, while it enhanced in G3 ($p<0.05$), G4, and G6 ($p>0.05$) (**Figure 7c**).

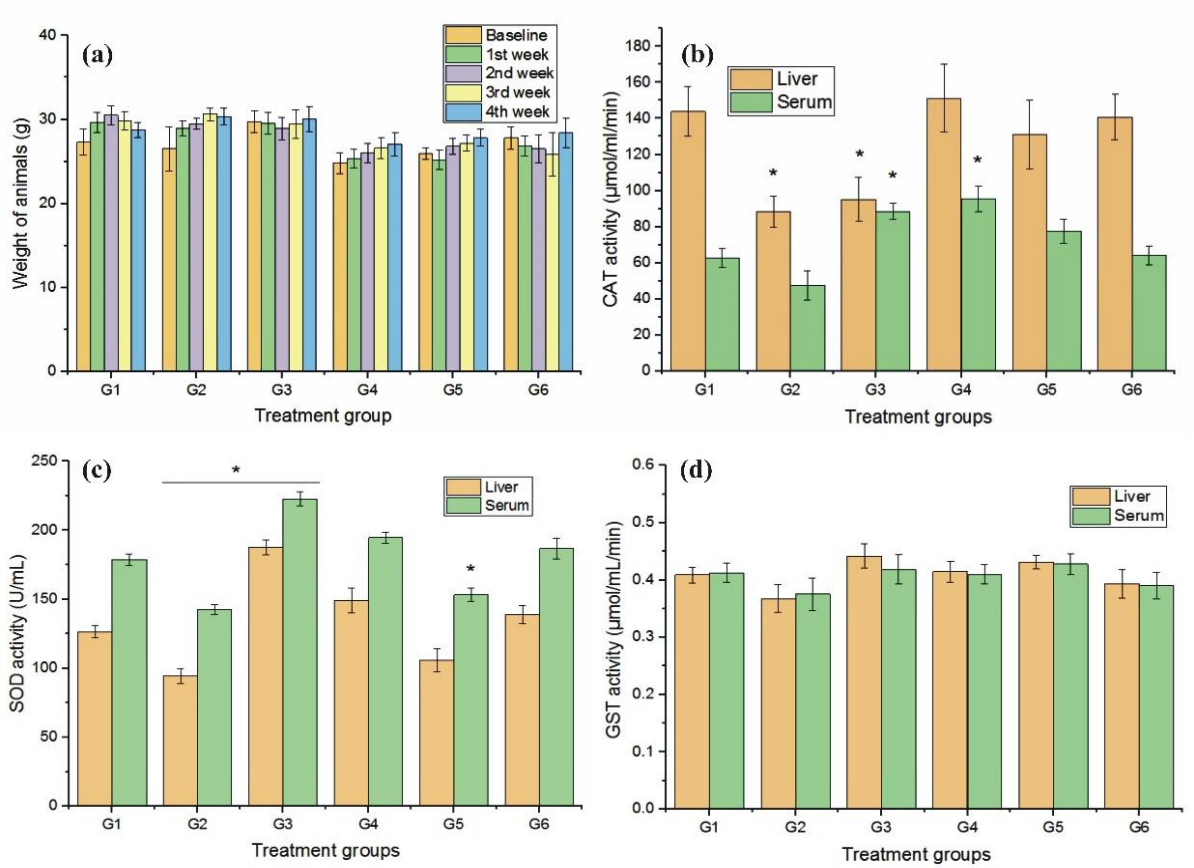

Figure 7. Exposure trial of AgNPrs and its conjugates; *(a)* animal body weight, *(b)* CAT-activity, For CAT, the data shown are Mean ± SE values (liver tissues $n = 5$, serum samples $n = 3$), for homogeneity of data ($p > 0.05$), a statistically significant difference was found in CAT activity among different groups, one-way ANOVA and Tukey test as post-hoc were conducted, where "*" indicates $p < 0.05$ when compared with control, *(c)* For SOD activity, the data shown are Mean ± SE values (liver tissues $n = 5$, serum samples $n = 3$), for homogeneity of data ($p > 0.05$), a statistically significant difference was found between different groups, one-way ANOVA followed by post- hoc Tukey test was applied, where "*" represent $p < 0.05$ when compared with control, *(d)* For GST, the data shown are Mean ± SE (liver tissues $n = 5$, serum samples $n = 3$), for homogeneity of data ($p > 0.05$), no statistically significant difference found in GST level between different groups, one-way ANOVA with post-hoc Tukey test was conducted; where G1 = control group supplied with saline water only, G2 = cadmium metal (20 mg/kg of the BW), G3 = Cadmium (20 mg/kg of BW) + C-AgNPrs (20 mg/kg of BW), G4 = Cadmium (20 mg/kg of BW) + Tyr-AgNPrs (20 mg/kg of BW), G5 = Cadmium (20 mg/kg of BW) + Gly-AgNPrs (20 mg/kg of BW), G6 = Cadmium (20 mg/kg of BW) + Cys-AgNPrs (20 mg/kg of BW).

Table 4: Body weight of the animals during the exposure period of NMs.

	Baseline	**1st week**	**2nd week**	**3rd week**	**4th week**
G1	27.325 ± 1.54	29.65 ± 1.19	30.5 ± 1.16	29.85 ± 1.14	28.75 ± 0.91
G2	26.55 ± 2.64	28.93 ± 0.90	29.5 ± 0.68	30.63 ± 0.74	30.36 ± 1.01
G3	29.78 ± 1.31	29.55 ±1.28	28.93 ± 1.36	29.48 ± 1.72	30.05 ± 1.52
G4	24.85 ± 1.26	25.33 ± 1.08	26.03 ± 1.14	26.63 ± 1.27	27.05 ± 1.37
G5	26.00 ± 0.69	25.20 ± 1.12	26.83 ± 0.94	27.18 ± 0.96	27.83 ± 1.01
G6	27.80 ± 1.36	26.85 ± 1.23	26.53 ± 1.68	25.90 ± 2.60	28.40 ± 1.72

Table 5: Comparison data of all the results obtained for cadmium metal (Cd), C-AgNPrs, and amino acids-capped AgNPrs.

Samples & Details	Cadmium	C-AgNPrs	Tyr-AgNPrs	Gly-AgNPrs	Cys-AgNPrs
Characterization					
UV-Vis-SPR peak	Not studied	980, 649, and 348nm	1093, negligible, 339nm	915, 632, 344nm	970, 654, 343nm
ZP Values	Not studied	-35.89 ± 1.14	-51.37 ± 1.01	-61.46 ± 2.45	-26.83 ± 1.78
Stability	Not studied	Over one year	Over one year	Over One year	Over 6 Months
FT-IR	Not studied	Not studied	$-NH_2$, -OH, -C-N, -C-H, -N-H	-N-H, -C-N, -C-H, C=O, COOH	-C=N, -C-N, -C-H, C-C=C-
Antioxidant activity (*in vitro*)					
DPPH	Not studied	Pro-oxidant	Enhanced Activity	Enhanced activity	Enhanced activity
FRP	Not studied	Mild-antioxidant	Reduced activity	Slightly reduced activity	Enhanced activity
HP	Not studied	Mild-antioxidant	Enhanced activity	Reduced activity	Enhanced activity
Antioxidant activity (*in vivo*)					
Catalase (µmol/ml/min) *	-38.68%	-33.76%	5.21%	-8.75%	-2.07%
SOD (U/mL) *	-25.30%	48.30%	18.07%	-16.13%	9.89%
GST (µmol/mL/min) *	-10.00%	8.04%	1.49%	5.62%	-3.72%
GSH in the kidney (µmol/g of tissue) *	0.37%	1.59%	1.89%	1.71%	1.77%
GSH in the liver (µmol/g of tissue) *	7.89%	2.26%	5.64%	4.15%	3.74%
MTs in the liver (µg/mg of the protein) *	5.07%	0.77%	-0.77%	0.29%	1.69%
MTs in the kidney (µg/mg of the protein) *	2.87%	0.58%	-1.12%	-0.14%	-0.29%

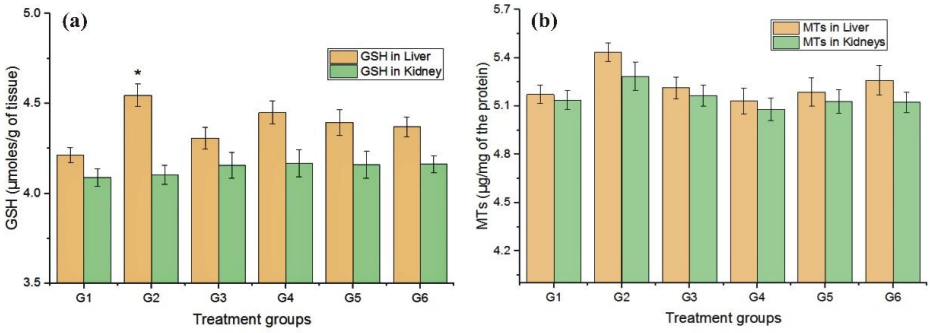

Figure 8. *(a)* For GSH level in the liver, the data shown are Mean ± SE values (liver tissue $n = 4$, kidney samples $n = 4$), for homogeneity of data ($p > 0.05$), a statistically significant difference in GSH level was present in liver tissues but not in kidney tissues, one-way ANOVA with posthoc Tukey test was applied, where "*" indicates $p < 0.05$ when compared with G1, *(b)* MTs level in tissues, the data shown are Mean ± SE values (liver tissues $n = 4$, kidney samples $n = 4$), for homogeneity of data ($p > 0.05$), no statistically significant difference was observed in both tissues in MTs between different groups, one-way ANOVA with Tukey test was conducted.

The G2 group displayed a slightly diminished (*p>0.05*) GST activity in serum and liver samples, while G3 and G5 groups exhibited a slightly increased activity. The G6 group showed a negligible change in activity compared to the control group (**Figure 7d**).

3.3.3. Metallothioneins (MTs) and reduced glutathione (GSH)

In liver and kidney tissue samples, GSH was increased in all treatment groups (G2-G6), however, it significantly increased in the liver tissue of the G2 group (*p>0.05*) in comparison to the G1 (**Figure 8a**). MTs were elevated in the G2 (*p>0.05*) in kidney and liver tissues, while in group G6 only liver tissues displayed enhanced production (*p>0.05*) of MTs (**Figure 8b**).

3.4. Synthesis of AgNPrs and their characterization

For the synthesis of AgNPrs, hydrogen peroxide-induced etching reaction on the surface plane of pre-formed AgNPs leads to a change in the surface morphology of NPs and yields prismatic AgNPrs. Furthermore, conjugation with amino acids depicted a slight change in the original peaks and color of AgNPrs (**Figure 1**). Jin *et al.* (2001) reported three distinct SPR peaks or AgNPrs, i.e., 340, 470, and 770 nm indicating the presence of out-of-plane quadrupole, in-plane quadrupole, and in-plane dipole plasmon resonance, respectively [48]. The peak at 770 nm also corresponds to the tips of the prisms [48, 4]. Sunder *et al.* (2022) suggested that silver nanospheres (Ag seeds) aggregated on proper planes to form AgNPrs [5]. Polarization of the conduction electrons in the plane parallel to the flat surface of nanoprisms corresponds to the presence of in-plane dipole plasmon resonance. Various other bands also develop due to the interaction of conduction band electrons with NPs [49, 50]. Chen *et al.* (2004) [51] also reported the synthesis of AgNPrs with an average edge size of 68 nm with four different SPR peaks, i.e., 352, 431, 465, and 552 nm, related to distinct planes. Contino *et al.* (2017) reported the synthesis of amino acid-capped anisotropic AgNPrs. The concentration of precursor salt influences the edge size and truncation of the tips of prismatic NMs [52].

Repeated UV visible studies revealed that the AgNPrs and their conjugates displayed more than one-year of stability except for Cys-AgNPrs (figure 4). Furthermore, the development of two distinct peaks in Cys-AgNPrs indicated a change in shape over time. Various functional groups present in amino acids are crucial in the capping and conjugation process. Few other studies with comparable results have been reported [53, 54]. After the synthesis of Cys-AgNPrs, different peaks of l-cystine on FTIR spectra were reduced or disappeared i.e., 1230, 1516, 1749, and 2355 cm^{-1} indicating the presence of C-N, -C-C=C, C=O, and C=N, respectively (**Figure 3a**). Various peaks of glycine, i.e., 1226, 1558, 1747, 2112, and 2355 cm^{-1} indicating to C-N, N-H, C=O, COOH, and C=N, respectively, were reduced or disappeared (**Figure 3b**). In Tyr-AgNPrs, several peaks at 840, 1043, 2351, 2644, 2933, 3207 cm^{-1} indicating to C-N, C=N, -OH, -N-H, and NH_2 were reduced or disappeared [55].

The net surface charge of molecules or nanoparticles is called zeta potential (ZP). Particles with higher negative ZP values seem to

be more stable. Gly-AgNPrs displayed the highest negative ZP values, whereas Cys-AgNPrs exhibited minimum values. Different interactions of molecules or nanoparticles with surfactants, such as polymers, or other biomolecules may alter zeta potential (ζ), i.e., dissociating different surface functional groups, shifting slipping planes, and displacing counter-ions [56]. These factors affect the ZP values of colloids or molecules. Various functional groups and their concerned ionic nature; negatively charged groups, e.g., -COOH, or, positively charged groups, e.g., $-NH_2$, assign negative or positive zeta potential, respectively [57].

Among all NMs, cystine-capped AgNPrs showed the lowest negative ZP values, which indicates their lower stability in colloidal solutions. It may be linked to the positively-charged group such as $-NH_2$ on the surface of AgNPrs. The pH of the colloidal solution also affects ZP values, as it influences intramolecular and intermolecular properties and interactions of the molecules [57, 58]. All silver nanoprisms were maintained at higher pH (7.4) than the corresponding isoelectric point (pI) of their amino acids. At higher pH values, the solution has a higher level of OH^- group, which helps to remove H^+ ions from positively-charged amine groups, which results in an overall negative thus having a negative zeta potential value [59]. Similarly, the samples of silver nanoprisms displayed negative charges. AgNPrs exhibited triangular-shaped (prismatic)-morphology with an average edge size of 63.40 ± 4.02 nm displaying three SPR peaks, i.e., 980, 649, and 348 nm. Silver nanospheres (Ag seeds) aggregated on proper planes to form AgNPrs [5]. Different bands also develop due to the interaction of conduction band electrons with the surface of NMs [49, 50].

3.5. In vitro antioxidants activity of NMs

Capping of tyrosine and cystine on AgNPrs enriched DPPH scavenging activity, while glycine further reduced it. Chemically-prepared AgNPrs showed pro-oxidant activity. According to Bedlovičová *et al.* (2020) [60] and Blois (1958) [61], DPPH is a radical that provides purple color in ethanol and accepts hydrogen atoms from an antioxidant or a scavenger molecule. Chemical-AgNPrs are very toxic, whereas their surface functionality with suitable biomolecules may reduce their toxicity. The enhanced antioxidant perspective of tyrosine and cystine conjugates might be associated with the phenolic group on tyrosine or the disulfide bond on cystine. No data are available to date on the DPPH scavenging activity of AgNPrs or their conjugates. Thus, it is the first report on the antioxidant activity of surface-modified AgNPrs.

Nanomaterials also displayed ferric-reducing power (FRP). Among all the nanoconjugates, Cys-AgNPrs exhibited higher FRP activity than the other nanoconjugates of silver nanoprisms. Chemically-synthesized silver nanoprisms also demonstrated FRP activity, but it was lower than the activity of Cys-AgNPrs but higher than Gly-AgNPrs. Increased absorbance of the mixture validates the high reducing power activity of the samples [62]. Silver conjugation with tyrosine and cystine displayed enhanced FRP activity. This activity measures the capacity of molecules to reduce ferric ions (Fe^{+3}) to ferrous ions (Fe^{+2}) [63]. Different functional groups of amino acids, when present on the surface of NMs

largely modulate redox and metal chelation reactions [64-66]; thus, influencing the FRP activity of AgNPrs.

Capping of tyrosine amino acids produced NMs with comparable hydrogen peroxide (HP) scavenging activity. Various biochemical pathways or enzymes generate hydrogen peroxide (as a by-product), which forms free radicals in high amounts resulting in the onset of oxidative stress [67, 68].

3.6. In vivo antioxidant activity

On exposure to AgNPrs, a slight increase in body weight (BW) was recorded in all the animal groups. Metabolism and nutritional uptake remain uninfluenced during the dosing period. Cadmium ions generally activated pro-survival signaling leading to the development of tumors and toxicity in the body [69-72]. Excessive orotic acid (OA) is generated during glycine metabolism, which promotes tumor development in some cases [73]. Another study by Zhang *et al.* (2012) [74] reported that the metabolism of glycine and serine is somewhere influenced by glycine decarboxylase (GLDC), and these changes in metabolic pathways further influence pyrimidine metabolism which further influences tumor development.

The body produces different types of antioxidant enzymes during metabolic activities. The kidney or liver clears them off using appropriate pathways and actions. Kidneys help to filter SOD, while hepatocytes of the liver clear catalase. Superoxide ions are converted into hydrogen peroxide (HP) in the presence of SOD, while HP changes to oxygen and water with the help of CAT. Glutathione-s-transferase (GST) help in the efficient disposal of xenobiotic from the body [32]. According to Jamakala and Rani (2015) [75], SOD, GST, and CAT activity was depressed in cadmium-exposed mice. Different factors influence alteration in antioxidant enzymes within the animal body including chemicals and their concentration, exposure time and route, and synthesis method. Wu and Zhou (2013) [76] reported that the decrease in endogenous enzymes might be linked to their higher consumption rate during oxidative stress.

Beytut and Aksakal (2002) [77] reported decreased production of CAT and higher production of ROS in cadmium-exposed mice. Saturation of free CAT by an increased level of hydrogen peroxide resulted in CAT shortage. The surface-functionality of AgNPrs resulted in different biological effects. Different functional groups present in AgNPrs modified the biochemical pathways differently, causing a deviation in the endogenous enzymes. The surface functionality of AgNPrs with cystine and tyrosine resulted in minor changes in the status of endogenous enzymes and induced negligible toxicity.

Glutathione-s-transferase shows a considerable physiological role in the detoxification of various molecules. The Thiol (-SH) group of GST molecule generally attaches with active agents of target molecules, and it neutralizes the electrophilic sites and makes highly water-soluble by-products. Exposure to nanomaterials makes a higher quantity of radical species and peroxides. Excessive utilization of GST results in decreased GST activity [78, 32]. Furthermore, reduced activity of GST may be linked with glutathione (GSH) affinity to NPs [79]. The synthesis of various complexes induces

glutathione oxidation and excessive generation of free radicals, which eventually results in diminished GST activity. Rajkumar et al. (2016) also reported comparable findings [80].

Decreased level of GSH is linked somewhere with a depressed immune response [81, 79], while An increased level of GSH in the cadmium-treated group (G2) might be associated with an increased immune response. Altered levels of MTs in different groups indicated metals-induced toxicity in liver and kidney tissues. Metallothionein levels in cadmium-intoxicated groups did not elevate in the presence of amino acids-capped AgNPrs. Metallothioneins (MTs) are highly important proteins with high cystinee content and low molecular weight. MTs are important in the detoxification of heavy metals and homeostasis [82, 83], and also play an important role during oxidative stress, infection, and inflammation [84, 85]. They may also work as sensitive biomarkers for various medical conditions such as cancer [82, 86].

Klaassen et al. (1999) reported a reduction in toxicity as a result of metal chelation with MTs in different organs [84]. Metallothioneins also facilitate GSH to maintain ROS balance in the body. Cystinee-rich residues of MTs work as binding sites for numerous metallic ions [87].

According to Atanesyan *et al.* (2011) [88], silver ions led to the up-regulation of MTs genes with the help of metal-responsive transcription factor-1 (MTF-1) binding metal-response elements (MRE). Smulders *et al.* (2015) reported the chelation reaction of NPs in the presence of other thiol-group-containing molecules and MTs [89]. Liver tissues are damaged in the presence of Cd, while MTs help to neutralize Cd and protect different organs [90]. Nordberg *et al.* (1975)[91] reported the kidney also as a target organ for cadmium toxicity. The formation of the cadmium-metallothioneins (Cd-MTs) complex further increase the toxicity in different organs of animals. Amino acid's capping largely instigated the level of MTs in the kidneys and liver, so the level of MTs were different in different groups for all types of exposure to AgNPrs. Cadmium-induced the generation of MTs in higher amounts, while conjugated amino acids help to revert-cadmium-induced toxicity and somewhere affected the production of metallothioneins. Generally, antioxidants reduce Cd absorption in the small intestine, and most of the ingested Cd is released along with fecal material resulting in a minimum reach of Cd to different tissues [92]. Tissue damage in the small intestine may impair the normal functioning of the intestine, such as absorption, digestion, and permeability thus influencing animal weight [93].

The surface functionality of AgNPrs with different amino acids may alter their optical, biological, and physicochemical properties, influencing their roles in biological systems. The interaction of various biomolecules or functional groups might help to reduce or alter toxicity [94]. Thiol group under specific conditions or disulfide (S-S) bond from cystine may play a crucial role [32]. In the case of the Cys-AgNPrs treatment group, it helps to reduce cadmium-induced toxicity, but further research is needed to clarify the context. Previous studies also reported the protective effects of cystine amino acids in mice [95, 96]. Several studies have also reported that the biomolecules conjugated AgNPs exhibited minimum toxicity [97, 98, 32], whereas the present study provides the first report on cystine-

capped-silver nanoprisms for their antioxidant potential in reverting cadmium toxicity in mice.

Surface functionality or surface modification of nanomaterials may yield environment-friendly and biocompatible nanomaterials. Biomolecule-mediated functionalization might produce effective, safer, and more secure nanomaterials for biomedical applications. These nanomaterials should be evaluated for their relative perspective for medical applications such as cancer therapy, medical imaging, and drug delivery. Nanomaterials with antioxidant potential may provide efficient, targeted delivery with higher stability and superior bioavailability. These molecules may overcome different limitations of small-molecule antioxidants. Molecular and gene expression studies should be undertaken to understand the detailed mechanisms of their action and response; which may help to design innovative materials with enhanced biodegradability and biocompatibility. Antioxidant nanomaterials might provide exceptional materials for biomedical applications and therapeutics; which can transform healthcare systems more innovatively.

4. Conclusion

Surface functionality of different metallic nanomaterials (NMs) using suitable biomolecules, such as amino acids, may enhance their safety profiling and make them more biocompatible and effective for their *in vivo* biological applications. During this study, amino acids capped silver nanoprisms were synthesized and characterized by using, UV-Visible spectroscopy, FTIR, zeta potential, etc. Cystine-AgNPrs and tyrosine-AgNPrs displayed enhanced *in vivo* and *in vitro* antioxidant properties. These results revealed that the cystine-AgNPrs and tyrosine-AgNPrs can be employed as effective nano-tools for various biological applications, but comprehensive profiling of these NMs is further needed to clarify their in-depth potential before using them for any practical and health-related application.

Acknowledgments

The authors are highly grateful to the Centre for Advanced Studies in Physics (CASP), Departments of Chemistry and Zoology, Government College University, Lahore, Pakistan. We are also highly thankful to LUMS University Lahore for their technical and moral support during this study. The authors also like to acknowledge the role of Ms. Zainab Hassan from the Department of Zoology, Government College University Lahore, and Mr. Muhammad Zubair from the University of Veterinary and Animal Sciences Lahore, for their kind support and facilitation.

Conflict of interest

The authors declare to have no conflict of interest.

References

[1]. Zhu Q-L, Xu Q (2016) Immobilization of ultrafine metal nanoparticles to high-surface-area materials and their catalytic applications. Chem 1 (2):220-245

[2]. Csapó E, Sebők D, Makrai Babić J, Šupljika F, Bohus G, Dékány I, Kallay N, Preočanin T (2014) Surface and structural properties of gold nanoparticles and their biofunctionalized derivatives in aqueous electrolytes solution. Journal of dispersion science and technology 35 (6):815-825

[3]. García MA (2011) Surface plasmons in metallic nanoparticles: fundamentals and applications. Journal of Physics D: Applied Physics 44 (28):283001

[4]. Banerjee S, Shyamsundar K, Saharay M, Roy S (2022) A single-step low cost detection of ground water Hg2+ using mercaptosuccinic acid functionalised silver nanoprism. Environmental Nanotechnology, Monitoring & Management 17:100637

[5]. Sundar KS, Ramesh J, Chinthala P, Rao K, Banerjee S, Roy S (2022) Silver nanoprism-mediated protein estimation—an ultrasensitive platform for rapid estimation of protein concentration. Nano Express 3 (2):025002

[6]. Yakoh A, Rattanarat P, Siangproh W, Chailapakul O (2018) Simple and selective paper-based colorimetric sensor for determination of chloride ion in environmental samples using label-free silver nanoprisms. Talanta 178:134-140

[7]. Jiang D, Tang B, Guo H, Xu W, Xu S (2013) Halide ions sensing in water via silver nanoprism self-assembled chips. Science of Advanced Materials 5 (8):1105-1110

[8]. Yen C-W, de Puig H, Tam JO, Gómez-Márquez J, Bosch I, Hamad-Schifferli K, Gehrke L (2015) Multicolored silver nanoparticles for multiplexed disease diagnostics: distinguishing dengue, yellow fever, and Ebola viruses. Lab on a Chip 15 (7):1638-1641

[9]. Shen J, Sun C, Wu X (2017) Silver nanoprisms-based Tb (III) fluorescence sensor for highly selective detection of dopamine. Talanta 165:369-376

[10]. Yuan M, Xiong Q, Zhang G, Xiong Z, Liu D, Duan H, Lai W (2020) Silver nanoprism-based plasmonic ELISA for sensitive detection of fluoroquinolones. Journal of materials chemistry B 8 (16):3667-3675

[11]. Hallaj T, Salari R, Amjadi M (2022) Morphology transition of Ag nanoprisms as a platform to design a dual sensor for NADH sensitive assay. Journal of Photochemistry and Photobiology A: Chemistry:114043

[12]. Rauf S, Hayat Nawaz MA, Badea M, Marty JL, Hayat A (2016) Nano-engineered biomimetic optical sensors for glucose monitoring in diabetes. Sensors 16 (11):1931

[13]. Dutta AK, Dutta NK (2022) Protein, Biomimetic Protein, and Designer Peptide-directed Synthesis of Metal Nanoparticles, Metal Nanoclusters and Nanobioconjugates, and Their Potential Applications. Biomimetic Protein Based Elastomers: Emerging Materials for the Future

[14]. Truong TTV, Chen C-C, Kumar SR, Hu C-C, Chen DW, Liu Y-K, Lue SJ (2022) Prismatic Silver Nanoparticles Decorated on Graphene Oxide Sheets for Superior Antibacterial Activity. Pharmaceutics 14 (5):924

[15]. Liang J, Yao C, Li X, Wu Z, Huang C, Fu Q, Lan C, Cao D, Tang Y (2015) Silver nanoprism etching-based plasmonic ELISA for the high sensitive detection of prostate-specific antigen. Biosensors and Bioelectronics 69:128-134

[16]. Wu D, Lu H-F, Xie H, Wu J, Wang C-M, Zhang Q-L (2015) Uricase-stimulated etching of silver nanoprisms for highly selective and sensitive colorimetric detection of uric acid in human serum. Sensors and Actuators B: Chemical 221:1433-1440

[17]. Mitra S, Basak M (2022) Diverse bio-sensing and therapeutic applications of plasmon enhanced nanostructures. Materials Today

[18]. Mout R, Moyano DF, Rana S, Rotello VM (2012) Surface functionalization of nanoparticles for nanomedicine. Chemical Society Reviews 41 (7):2539-2544

[19]. Chou LY, Ming K, Chan WC (2011) Strategies for the intracellular delivery of nanoparticles. Chemical Society Reviews 40 (1):233-245

[20]. Saha K, Bajaj A, Duncan B, Rotello VM (2011) Beauty is Skin Deep: A Surface Monolayer Perspective on Nanoparticle Interactions with Cells and Bio-macromolecules. Small 7 (14):1903-1918

[21]. Elghanian R, Storhoff JJ, Mucic RC, Letsinger RL, Mirkin CA (1997) Selective colorimetric detection

of polynucleotides based on the distance-dependent optical properties of gold nanoparticles. Science 277 (5329):1078-1081

[22]. Hoffman AS (2008) The origins and evolution of "controlled" drug delivery systems. Journal of controlled release 132 (3):153-163

[23]. Ahmad F, Salem-Bekhit MM, Khan F, Alshehri S, Khan A, Ghoneim MM, Wu H-F, Taha EI, Elbagory I (2022) Unique Properties of Surface-Functionalized Nanoparticles for Bio-Application: Functionalization Mechanisms and Importance in Application. Nanomaterials 12 (8):1333

[24]. Preiss LC, Wagner M, Mastai Y, Landfester K, Muñoz-Espí R (2016) Amino-Acid-Based Polymerizable Surfactants for the Synthesis of Chiral Nanoparticles. Macromolecular Rapid Communications 37 (17):1421-1426

[25]. Infante M, Pinazo A, Seguer J (1997) Non-conventional surfactants from amino acids and glycolipids: structure, preparation and properties. Colloids and Surfaces A: Physicochemical and Engineering Aspects 123:49-70

[26]. Pinazo A, Pons R, Pérez L, Infante MR (2011) Amino acids as raw material for biocompatible surfactants. Industrial & Engineering Chemistry Research 50 (9):4805-4817

[27]. Xu C, Liu X, Xie B, Yao C, Hu W, Li Y, Li X (2016) Preparation of PES ultrafiltration membranes with natural amino acids based zwitterionic antifouling surfaces. Applied Surface Science 385:130-138

[28]. Qu H, Ma H, Zhou W, O'Connor CJ (2012) In situ surface functionalization of magnetic nanoparticles with hydrophilic natural amino acids. Inorganica Chimica Acta 389:60-65

[29]. Mandal S, Phadtare S, Sastry M (2005) Interfacing biology with nanoparticles. Current Applied Physics 5 (2):118-127

[30]. Patel D, Chang Y, Lee GH (2009) Amino acid functionalized magnetite nanoparticles in saline solution. Current Applied Physics 9 (1):S32-S34

[31]. Majzik A, Fülöp L, Csapó E, Bogár F, Martinek T, Penke B, Bíró G, Dékány I (2010) Functionalization of gold nanoparticles with amino acid, β-amyloid peptides and fragment. Colloids and Surfaces B: Biointerfaces 81 (1):235-241

[32]. Ditta SA, Yaqub A, Ullah R, Tanvir F (2021) Evaluation of amino acids capped silver nanoconjugates for the altered oxidative stress and antioxidant potential in albino mice. Journal of Materials Research 36 (21):4344-4359

[33]. Frank AJ, Cathcart N, Maly KE, Kitaev V (2010) Synthesis of silver nanoprisms with variable size and investigation of their optical properties: a first-year undergraduate experiment exploring plasmonic nanoparticles. Journal of Chemical Education 87 (10):1098-1101

[34]. Tanvir F, Yaqub A, Tanvir S, Anderson WA (2017) Poly-L-arginine coated silver nanoprisms and their anti-bacterial properties. Nanomaterials 7 (10):296

[35]. Shang Y, Wu F, Qi L (2012) Highly selective colorimetric assay for nickel ion using N-acetyl-l-cystinee-functionalized silver nanoparticles. Journal of Nanoparticle Research 14 (10):1-7

[36]. Shankar S, Rhim J-W (2015) Amino acid mediated synthesis of silver nanoparticles and preparation of antimicrobial agar/silver nanoparticles composite films. Carbohydrate polymers 130:353-363

[37]. Bhakya S, Muthukrishnan S, Sukumaran M, Muthukumar M (2016) Biogenic synthesis of silver nanoparticles and their antioxidant and antibacterial activity. Applied Nanoscience 6 (5):755-766

[38]. Sharifi-Rad J, Hoseini-Alfatemi S, Sharifi-Rad M, Iriti M (2014) Antimicrobial synergic effect of Allicin and silver nanoparticles on skin infection caused by methicillin resistant Staphylococcus aureus spp. Annals of medical and health sciences research 4 (6):863-868

[39]. Sharifi-Rad M, Pohl P, Epifano F, Álvarez-Suarez JM (2020) Green Synthesis of Silver Nanoparticles Using Astragalus tribuloides Delile. Root Extract: Characterization, Antioxidant, Antibacterial, and Anti-Inflammatory Activities. Nanomaterials 10 (12):2383

[40]. Jayaprakasha GK, Singh R, Sakariah K (2001) Antioxidant activity of grape seed (Vitis vinifera)

extracts on peroxidation models in vitro. Food chemistry 73 (3):285-290

[41]. Keshari AK, Srivastava A, Verma AK, Srivastava R (2016) Free radicals scavenging and protein protective property of Ocimum sanctum (L). British Journal of Pharmaceutical Research 14 (4):1-10

[42]. Co-operation OfE, Development (2008) Test No. 407: repeated dose 28-day oral toxicity study in rodents. OECD Publishing,

[43]. Marklund S, Marklund G (1974) Involvement of the superoxide anion radical in the autoxidation of pyrogallol and a convenient assay for superoxide dismutase. European journal of biochemistry 47 (3):469-474

[44]. Javed M, Usmani N, Ahmad I, Ahmad M (2015) Studies on the oxidative stress and gill histopathology in Channa punctatus of the canal receiving heavy metal-loaded effluent of Kasimpur Thermal Power Plant. Environmental monitoring and assessment 187 (1):4179

[45]. Roy S, Bhattacharya S (2006) Arsenic-induced histopathology and synthesis of stress proteins in liver and kidney of Channa punctatus. Ecotoxicology and Environmental Safety 65 (2):218-229

[46]. Delmond KA, Vicari T, Guiloski IC, Dagostim AC, Voigt CL, de Assis HCS, Ramsdorf WA, Cestari MM (2019) Antioxidant imbalance and genotoxicity detected in fish induced by titanium dioxide nanoparticles (NpTiO2) and inorganic lead (PbII). Environmental toxicology and pharmacology 67:42-52

[47]. Viarengo A, Ponzano E, Dondero F, Fabbri R (1997) A simple spectrophotometric method for metallothionein evaluation in marine organisms: an application to Mediterranean and Antarctic molluscs. Marine Environmental Research 44 (1):69-84

[48]. Jin R, Cao Y, Mirkin CA, Kelly KL, Schatz GC, Zheng J (2001) Photoinduced conversion of silver nanospheres to nanoprisms. science 294 (5548):1901-1903

[49]. Bastys V, Pastoriza-Santos I, Rodríguez-González B, Vaisnoras R, Liz-Marzán LM (2006) Formation of silver nanoprisms with surface plasmons at communication wavelengths. Advanced Functional Materials 16 (6):766-773

[50]. Hao E, Schatz GC, Hupp JT (2004) Synthesis and optical properties of anisotropic metal nanoparticles. Journal of fluorescence 14 (4):331-341

[51]. Chen S, Webster S, Czerw R, Xu J, Carroll DL (2004) Morphology effects on the optical properties of silver nanoparticles. Journal of Nanoscience and Nanotechnology 4 (3):254-259

[52]. Contino A, Maccarrone G, Zimbone M, Seggio M, Musumeci P, Giuffrida A, Calcagno L (2017) Synthesis and characterization of new tyrosine capped anisotropic silver nanoparticles and their exploitation for the selective determination of iodide ions. Colloids and Surfaces A: Physicochemical and Engineering Aspects 529:128-136

[53]. Ijaz M, Zafar M, Iqbal T (2020) Green synthesis of silver nanoparticles by using various extracts: a review. Inorganic and Nano-Metal Chemistry:1-12

[54]. Rajput S, Kumar D, Agrawal V (2020) Green synthesis of silver nanoparticles using Indian Belladonna extract and their potential antioxidant, anti-inflammatory, anticancer and larvicidal activities. Plant Cell Reports 39 (7):1-19

[55]. Hemmalakshmi S, Priyanga S, Devaki K (2017) Fourier Transform Infra-Red Spectroscopy Analysis of Erythrina variegata L. Journal of Pharmaceutical Sciences and Research 9 (11):2062-2067

[56]. Vincent B (1974) The effect of adsorbed polymers on dispersion stability. Advances in Colloid and Interface Science 4 (2-3):193-277

[57]. Ostolska I, Wiśniewska M (2014) Application of the zeta potential measurements to explanation of colloidal Cr 2 O 3 stability mechanism in the presence of the ionic polyamino acids. Colloid and polymer science 292 (10):2453-2464

[58]. Wiśniewska M, Szewczuk-Karpisz K (2013) Removal possibilities of colloidal chromium (III) oxide from water using polyacrylic acid. Environmental Science and Pollution Research 20 (6):3657-3669

[59]. Regenstein J, Regenstein C (1984) Protein Functionality for Food Scientists In Food Protein Chemistry. Florida. Academic Press Inc,

[60]. Bedlovičová Z, Strapáč I, Baláž M, Salayová A (2020) A brief overview on antioxidant activity

determination of silver nanoparticles. Molecules 25 (14):3191

[61]. Blois MS (1958) Antioxidant determinations by the use of a stable free radical. Nature 181 (4617):1199-1200

[62]. Alam MN, Bristi NJ, Rafiquzzaman M (2013) Review on in vivo and in vitro methods evaluation of antioxidant activity. Saudi pharmaceutical journal 21 (2):143-152

[63]. Shelembe B, Mahlangeni NT, Moodley R (2019) Biosynthesis of gold nanoparticles using monosaccharides of Artemisia afra and their antioxidant and anticancer properties. Advances in Natural Sciences: Nanoscience and Nanotechnology 10 (4):045002

[64]. Deneke SM (2001) Thiol-based antioxidants. Current topics in cellular regulation 36:151-180

[65]. Giles NM, Watts AB, Giles GI, Fry FH, Littlechild JA, Jacob C (2003) Metal and redox modulation of cystinee protein function. Chemistry & biology 10 (8):677-693

[66]. Kim J-H, Jang H-J, Cho W-Y, Yeon S-J, Lee C-H (2020) In vitro antioxidant actions of sulfur-containing amino acids. Arabian Journal of Chemistry 13 (1):1678-1684

[67]. Chang H-F, Yang L-L (2012) Radical-scavenging and rat liver mitochondria lipid peroxidative inhibitory effects of natural flavonoids from traditional medicinal herbs. Journal of Medicinal Plants Research 6 (6):997-1006

[68]. Gülçin I (2007) Comparison of in vitro antioxidant and antiradical activities of L-tyrosine and L-Dopa. Amino acids 32 (3):431-438

[69]. Arroyo V, Flores K, Ortiz L, Gómez-Quiroz L, Gutiérrez-Ruiz M (2012) Liver and cadmium toxicity. J Drug Metab Toxicol S 5 (001)

[70]. Jing Y, Liu L-Z, Jiang Y, Zhu Y, Guo NL, Barnett J, Rojanasakul Y, Agani F, Jiang B-H (2012) Cadmium increases HIF-1 and VEGF expression through ROS, ERK, and AKT signaling pathways and induces malignant transformation of human bronchial epithelial cells. Toxicological sciences 125 (1):10-19

[71]. Thévenod F, Lee W-K (2013) Cadmium and cellular signaling cascades: interactions between cell death and survival pathways. Archives of toxicology 87 (10):1743-1786

[72]. Wei T, Jia J, Wada Y, Kapron CM, Liu J (2017) Dose dependent effects of cadmium on tumor angiogenesis. Oncotarget 8 (27):44944

[73]. Vasudevan S, Laconi E, Abanobi SE, Rao PM, Rajalakshmi S, Sarma DS (1987) Effect of glycine on the induction of orotic aciduria and urinary bladder tumorigenesis in the rat. Toxicologic pathology 15 (2):194-197

[74]. Zhang H, Ji Z, Xia T, Meng H, Low-Kam C, Liu R, Pokhrel S, Lin S, Wang X, Liao Y-P (2012) Use of metal oxide nanoparticle band gap to develop a predictive paradigm for oxidative stress and acute pulmonary inflammation. ACS nano 6 (5):4349-4368

[75]. Jamakala O, Rani UA (2015) Amelioration effect of zinc and iron supplementation on selected oxidative stress enzymes in liver and kidney of cadmium-treated male albino rat. Toxicology International 22 (1):1

[76]. Wu Y, Zhou Q (2013) Silver nanoparticles cause oxidative damage and histological changes in medaka (Oryzias latipes) after 14 days of exposure. Environmental Toxicology and Chemistry 32 (1):165-173

[77]. Beytut E, Aksakal M (2002) The effect of long-term supplemental dietary cadmium on lipid peroxidation and the antioxidant system in the liver and kidneys of rabbits. Turkish Journal of Veterinary and Animal Sciences 26 (5):1055-1060

[78]. Boulahia K, Carol P, Planchais Sv, Abrous-Belbachir O (2016) Phaseolus vulgaris L. seedlings exposed to prometryn herbicide contaminated soil trigger an oxidative stress response. Journal of agricultural and food chemistry 64 (16):3150-3160

[79]. Morris D, Khurasany M, Nguyen T, Kim J, Guilford F, Mehta R, Gray D, Saviola B, Venketaraman V (2013) Glutathione and infection. Biochimica et Biophysica Acta (BBA)-General Subjects 1830 (5):3329-3349

[80]. Rajkumar K, Kanipandian N, Thirumurugan R (2016) Toxicity assessment on haemotology, biochemical and histopathological alterations of silver nanoparticles-exposed freshwater fish Labeo rohita. Applied Nanoscience 6 (1):19-29

[81]. Dröge W, Breitkreutz R (2000) Glutathione and immune function. Proceedings of the Nutrition Society 59 (4):595-600

[82]. Albrecht AL, Singh RK, Somji S, Sens MA, Sens DA, Garrett SH (2008) Basal and metal-induced expression of metallothionein isoform 1 and 2 genes in the RWPE-1 human prostate epithelial cell line. Journal of Applied Toxicology: An International Journal 28 (3):283-293

[83]. Coyle P, Philcox J, Carey L, Rofe A (2002) Metallothionein: the multipurpose protein. Cellular and Molecular Life Sciences CMLS 59 (4):627-647

[84]. Klaassen CD, Liu J, Choudhuri S (1999) Metallothionein: an intracellular protein to protect against cadmium toxicity. Annual review of pharmacology and toxicology 39 (1):267-294

[85]. Vallee BL (1995) The function of metallothionein. Neurochemistry international 27 (1):23-33

[86]. Rodrigo MAM, Jimemez AMJ, Haddad Y, Bodoor K, Adam P, Krizkova S, Heger Z, Adam V (2020) Metallothionein isoforms as double agents–Their roles in carcinogenesis, cancer progression and chemoresistance. Drug Resistance Updates 52:100691

[87]. Liu J, Hu X, Hou S, Wen T, Liu W, Zhu X, Yin J-J, Wu X (2012) Au@ Pt core/shell nanorods with peroxidase-and ascorbate oxidase-like activities for improved detection of glucose. Sensors and Actuators B: Chemical 166:708-714

[88]. Atanesyan L, Günther V, Celniker SE, Georgiev O, Schaffner W (2011) Characterization of MtnE, the fifth metallothionein member in Drosophila. JBIC Journal of Biological Inorganic Chemistry 16 (7):1047-1056

[89]. Smulders S, Larue C, Sarret G, Castillo-Michel H, Vanoirbeek J, Hoet PH (2015) Lung distribution, quantification, co-localization and speciation of silver nanoparticles after lung exposure in mice. Toxicology letters 238 (1):1-6

[90]. Goering PL, Klaassen CD (1984) Tolerance to cadmium-induced toxicity depends on presynthesized metallothionein in liver. Journal of Toxicology and Environmental Health, Part A Current Issues 14 (5-6):803-812

[91]. Nordberg G, Goyer R, Nordberg M (1975) Comparative toxicity of cadmium-metallothionein and cadmium chloride on mouse kidney. Archives of pathology 99 (4):192-197

[92]. Zhai Q, Wang G, Zhao J, Liu X, Tian F, Zhang H, Chen W (2013) Protective effects of Lactobacillus plantarum CCFM8610 against acute cadmium toxicity in mice. Applied and environmental microbiology 79 (5):1508-1515

[93]. He X, Qi Z, Hou H, Qian L, Gao J, Zhang X-X (2020) Structural and functional alterations of gut microbiome in mice induced by chronic cadmium exposure. Chemosphere 246:125747

[94]. Chakraborty A, Boer JC, Selomulya C, Plebanski M (2017) Amino acid functionalized inorganic nanoparticles as cutting-edge therapeutic and diagnostic agents. Bioconjugate chemistry 29 (3):657-671

[95]. Gaurav D, Preet S, Dua K (2010) Chronic cadmium toxicity in rats: treatment with combined administration of vitamins, amino acids, antioxidants and essential metals. Journal of Food and Drug Analysis 18 (6):464-470

[96]. Shoji K, Yuri M, Toshiya H, Morio K, Hideaki S, Takayuki F (1992) Effect of L-cystine on toxicity of paraquat in mice. Toxicology letters 60 (1):75-82

[97]. Kim B, Han G, Toley BJ, Kim C-k, Rotello VM, Forbes NS (2010) Tuning payload delivery in tumour cylindroids using gold nanoparticles. Nature nanotechnology 5 (6):465-472

[98]. Sung JH, Ji JH, Park JD, Yoon JU, Kim DS, Jeon KS, Song MY, Jeong J, Han BS, Han JH (2009) Subchronic inhalation toxicity of silver nanoparticles. Toxicological sciences 108 (2):452-461.